

Bright atomic beam by a temporal Zeeman acceleration

Y. Fukuyama¹, H. Kanou¹, V.I. Balykin^{1,2}, K. Shimizu¹

¹Institute for Laser Science, University of Electro-Communications, Chofu-shi, Tokyo 182-8585, Japan
(Fax: +81-424/85-8960, E-mail: y_fukuya@ils.uec.ac.jp)

²Institute of Spectroscopy, Russian Academy of Science, 142092 Troitsk, Moscow Region, Russia

Received: 22 October 1999/Revised version: 15 November 1999/Published online: 8 March 2000 – © Springer-Verlag 2000

Abstract. A novel method to produce a slow, monochromatic, and bright pulsed atomic beam from a magneto-optical trap by switching the magnetic field of the trap is proposed. A pulsed lithium atomic beam with a brightness of 1.1×10^{15} /sr s and a velocity of 13 m/s was produced as an experimental proof of this technique. The conversion efficiency from the trap into the atomic pulse was nearly 100%.

PACS: 32.80.Pj

There is a considerable interest in the generation of a slow atomic beam having a narrow velocity spread (SABNVS) that can be used in various experiments in physics such as ultrahigh resolution atomic and molecular spectroscopy, atom optics, atom interferometry, study of solid surfaces, and low-energy collision experiments. Before the invention of laser cooling the SABNVS was obtained by slicing out the low velocity component of the velocity distribution in a beam that has a broad Maxwell–Boltzmann distribution. This resulted in a poor brightness of the atomic beam.

After the invention of laser cooling several techniques were developed, which resulted in considerable improvement of the brightness. A most straightforward method is to decelerate the atomic beam with a set of properly detuned laser beams that counterpropagate against the atomic beam [1, 2]. However, a long distance is needed to slow down a significant portion of the atoms in the beam, and the process is accompanied inevitably by the transverse heating which decreases the brightness of the beam. More advanced techniques to overcome such difficulties were developed by using the trapping technique of neutral atoms. Riis et al. [3] confined and cooled a sodium atomic beam in the transverse direction using a two-dimensional magneto-optical trap (MOT). The device was called an atomic funnel. Similar experiments of two-dimensional atomic beam compression were reported by Nellesen et al. [4] on sodium, by Yu et al. [5] on cesium, and by Swanson et al. [6] on rubidium. The brightness of 3×10^{11} atoms/sr s at the velocity of 2.7 m/s was reported for the sodium beam [3]. For the metastable neon beam the brightness was 3×10^{10} atoms/sr s at the velocity of 19 m/s [7]. Although the finite flight time of atoms through the two-dimensional MOT limits the degree of velocity compression, this technique has been used to reduce the beam

divergence of atomic beam even at a higher velocity. An alternative technique is to extract atoms from a three-dimensional MOT. The advantage of this method is that the phase space density of atoms in a MOT is very large and that the loading time of the MOT can be reduced to a fraction of a second. Lu et al. [8] generated a continuous rubidium atomic beam with the flux of 5×10^9 atoms/s. When it was operated in the pulsed mode the flux increased by 10 times. The brightness of the beam was 5×10^{12} atoms/sr s in the continuous mode. A continuous beam of cold cesium atoms was generated also from a two-dimensional MOT, which produced a flux of 10^6 atoms/s [9].

In this paper we propose and demonstrate experimentally a novel method to produce a SABNVS. We obtained the atomic beam with the brightness of 1.1×10^{15} atoms/sr s at any average velocity below 13 m/s.

1 Principle of atomic beam formation

An atomic cloud in a three-dimensional magneto-optical trap was extracted from the trap by introducing imbalance of the trapping force by changing the trapping laser intensity and the magnetic field. The feature of this technique was that the atomic cloud was accelerated in a temporally varying magnetic field in one direction without large spreading of the cloud along the other directions. The configuration of our magneto-optical trap is illustrated in Fig. 1. The spherical quadrupole magnetic field was generated by two coils that were placed along the z axis at equal distance from the center of the trap and having opposite current directions. It produced linear magnetic field gradient around the center. Four laser beams generated three-dimensional centripetal force to confine atoms in the trap [10]. (The tetrahedral laser beam configuration was not essential in our method.) The three trapping laser beams (beams 2,3,4) accelerated the trapped atoms along the z axis, once the trapping beam 1 was switched off. While the atoms moved away from the center of the trap, the rate of the absorption of the accelerating laser beams decreased as a result of the increasing velocity-induced Doppler shift and the decreasing magnetic field. The resonance frequency of a two-level atom moving along the z axis is shifted by the Zeeman and the Doppler effects by $\Delta = \omega_L - \omega_0 + \mu_B B(z)/\hbar - \vec{k} \cdot \vec{v}(z, t)$, where ω_L is the laser

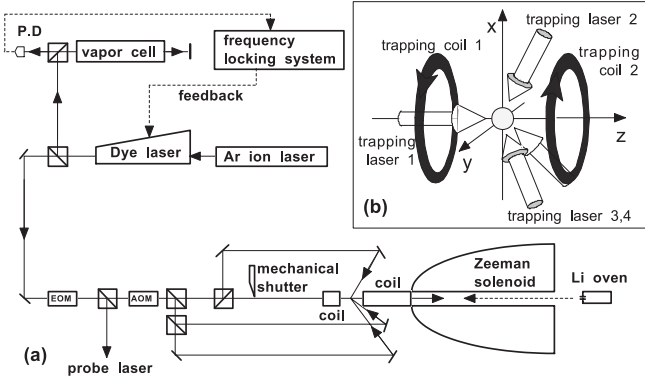


Fig. 1a,b. Schematic diagram of experimental setup (a) and MOT with the tetrahedral laser beam configuration (b). To accelerate atoms in the MOT the trapping laser 1 and the current to the trapping coil 1 were switched off simultaneously

frequency tuned below the atomic resonance frequency ω_0 . $B(z)$ is the magnetic field distribution along the z axis and is negative in $z < 0$ (downstream of the atomic beam). To keep the atoms on resonance with the fixed-frequency laser, we increased temporally the magnetic field in the downstream, simply by switch off the current in the downstream coil. The time constant of the changing magnetic field determined the acceleration. We have estimated the final velocity of the accelerated atoms when the magnetic field distribution $B(z)$ varied exponentially. It was around 20 m/s after acceleration of 1 ms in our experimental conditions. The final velocity of the atomic cloud was set by adjusting the duration of the acceleration, simply by turning off the three trapping laser beams at a specific time. The three trapping beams and the transverse magnetic field confined atoms transversely during the acceleration, resulting in the formation of a bright pulsed atomic beam.

2 Experiments

The experiments were performed on a sample of Li atoms confined in a MOT. The trap consisted of two coils which generated the spherical quadrupole magnetic field and four laser beams in the tetrahedral configuration described in our previous work [11]. The tetrahedral laser beam configuration gave a high capture ratio of decelerated atoms and ensured a large total number of trapped atoms. The trap was loaded from the atomic beam slowed by the Zeeman tuning technique. In the tetrahedral configuration, one of the trapping beam (laser beam 1) was directed towards the atomic beam source to use it also as a slowing beam. The trapping and cooling laser beams were supplied by a ring dye laser (Coherent CR699) pumped by an Ar-ion laser. The frequency of the dye laser was locked to the zero point of the first derivative of the saturated absorption spectrum of the cooling transition $^2S_{1/2}(F=2) - ^2P_{3/2}(F=3)$ ($\lambda = 671$ nm) using a lithium vapor cell.

In the present experiment, the long-term frequency stability was within 50 kHz/h, and the frequency jitter was typically 2 MHz. The laser frequency was tuned 15 MHz below the resonance of the cooling transition by applying dc magnetic field to the vapor cell. To avoid the optical

pumping into the another ground-state hyperfine component, the laser beam was modulated by an electro-optic modulator to generate sidebands at the frequency of ± 820 MHz. The upper sideband was resonant with the frequency of the $^2S_{1/2}(F=1) - ^2P_{3/2}(F=2)$ transition, and the atoms in the $^2S_{1/2}(F=1)$ state were optically pumped back to the cooling cycle. The intensity ratio of the sideband to the carrier was 1:3. The total intensity of the four laser beams was 6.8 mW/cm² including the sidebands (the saturation intensity of the cooling transition is 2.4 mW/cm²). The $1/e^2$ laser beam diameter at the trap was 20 mm. The number of atoms in a MOT was estimated from the fluorescence intensity and the trapping laser power density. The number of trapped atoms was typically 5×10^9 , the $1/e^2$ diameter of the atomic cloud was 3.3 mm, and the density was 1.5×10^{11} /cm³ when the magnetic field gradient along the z axis was 12 G/cm. The temperature of atomic cloud was measured by the time-of-flight method, and it was 1.9 mK. The loading time of the MOT was 300 ms, when the background gas pressure of the trapping chamber was 3×10^{-10} Torr and the temperature of the lithium oven was 900 K.

The atomic cloud was extracted from the MOT by shutting off the longitudinal trapping laser beam (beam 1) by a mechanical shutter. Simultaneously, the current through the downstream coil was switched off. The current decayed with the time constant of 0.3 ms and the magnetic field increased. Atoms were accelerated towards the $-z$ direction in the temporally varying magnetic field. The acceleration stopped when the remaining three trapping laser beams (beams 2,3,4) were turned off by an acousto-optic modulator. We call the period between the time to shut off the beam 1 and the beams 2,3,4 the acceleration time, τ_a . The acceleration time was precisely controlled using the acousto-optic modulator. The acceleration time τ_a was varied from 25 μ s to 1.2 ms. Its maximum value was limited by the time at which the accelerating atoms escape from the trapping laser beams.

The properties of the pulsed atomic beam were measured by two methods; the time of flight (TOF) and the imaging of atomic pattern. The TOF spectrum was measured with a resonant probe laser beam which crossed the z axis at the distance of 13 mm from the center of the MOT. The probe beam was focused by a cylindrical lens to a light sheet with the thickness of 250 μ m. Its width was 8 mm. The power density of the probe was 100 mW/cm². The fluorescence from the atomic cloud at the region of the probe beam was collected by a standard camera lens ($f = 50$ mm, $F/2$) and detected by a photomultiplier. Since the distance of 13 mm from the center of the MOT to the probe beam was not sufficiently long compared to a typical diameter of the atomic cloud, the data of TOF measurement were fitted by the following equation, which take into account of the initial spatial distribution of the cloud:

$$I(t) = \frac{N_0}{(\pi v w)^3 t^4} \int_{-3w}^{3w} dz \int_{d-l}^{d-l+\Delta l} dz' \exp \left[- \left(\frac{z}{w} \right)^2 \right] \times \exp \left[- \left(\frac{z' - z}{t \delta v} - \frac{v}{\delta v} \right)^2 \right], \quad (1)$$

where d is the distance between the probe beam and the center of the MOT, v is the average velocity, δv is the velocity

spread, w is the radius of $1/e^2$ atomic cloud, Δl is the thickness of the probe beam, and l is the acceleration distance.

To measure the spatial property of the pulsed atomic beam, the fluorescence image of the atomic cloud was recorded using a CCD camera equipped with an image intensifier. The vertical deflection signal (VD signal) that was extracted from the video signal was used as a clock pulse for the timing of the whole procedure of the formation of the atomic beam and the measurement of its properties. Using a camera lens with a small f -number and the intensifier with 10^4 gain, the pattern of the atomic cloud was recorded with $10\ \mu\text{s}$ temporal resolution. A high-voltage $10\text{-}\mu\text{s}$ gate pulse was applied on the photocathode of the intensifier synchronously to one frame of CCD camera. All parameters of the pulsed atomic beam were determined from two fluorescence images of the atomic cloud, one at the end of the acceleration and the other at a time after the acceleration followed by free flight. The second image was recorded using a standing wave probe beam with $10\ \text{mm}$ diameter and $1.2\ \text{mW}/\text{cm}^2$ power density that crossed the z axis $15\ \text{mm}$ downstream from the center of the MOT.

3 Results and discussions

3.1 Time-of-flight method

The velocity and velocity spread of the pulsed atomic beam were measured by the TOF method. Figure 2 shows a typical time-of-flight signal and fitting curve calculated from (1) in the case of $200\ \mu\text{s}$ acceleration which gives $3.3\ \text{m/s}$ average velocity and $1.0\ \text{m/s}$ velocity spread. The accuracy of determining the velocity and the velocity spread were $0.2\ \text{m/s}$ and $0.1\ \text{m/s}$, respectively. A series of time-of-flight signals at different acceleration times are shown in Fig. 3. The lowest curve is the signal without acceleration. The number of atoms in a pulse was nearly the same in four curves. The dynamics of formation of the pulsed atomic beam can be clearly seen from these curves. The oscilloscope trace was triggered by the signal from the mechanical shutter at the beginning of the acceleration. The small signal at the beginning of the trace, which came from the scattered trapping laser beam, indicates

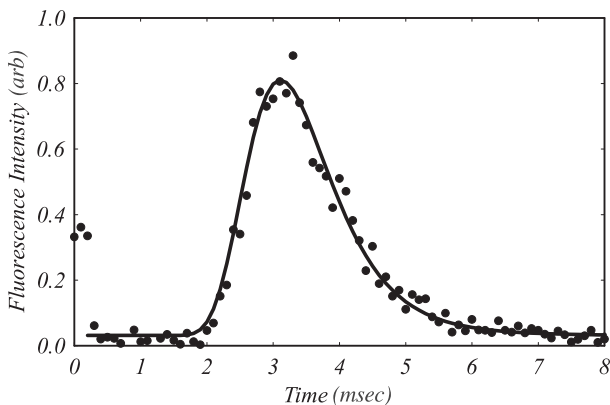


Fig. 2. A time-of-flight signal after the acceleration of $200\ \mu\text{s}$. The solid curve is the theoretical curve in which the parameters were determined from the experimental curve. The longitudinal velocity is $3.3\ \text{m/s}$ and the velocity spread is $1.0\ \text{m/s}$

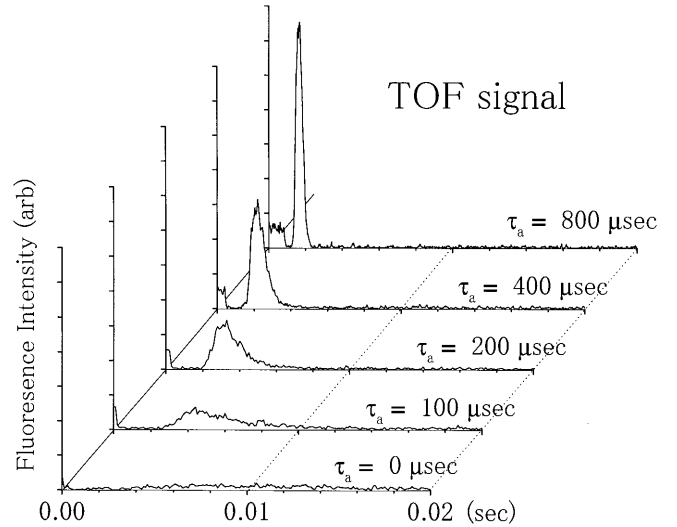


Fig. 3. Signals of the time-of-flight measurements of the pulsed atomic beams with and without acceleration. Acceleration times were $100\ \mu\text{s}$, $200\ \mu\text{s}$, $400\ \mu\text{s}$, $800\ \mu\text{s}$, respectively

the duration of the acceleration. The average velocity and the relative velocity spread as a function of acceleration time τ_a is shown in Fig. 4. When the acceleration time was varied from $100\ \mu\text{s}$ to $800\ \mu\text{s}$ the average velocity increased from $1.5\ \text{m/s}$ to $9\ \text{m/s}$.

3.2 Imaging method

The fluorescence images of atomic clouds were recorded to obtain the information of the position and the spatial distribution of atoms in the cloud after the acceleration. Figure 5 shows a series of images of the atomic cloud at different times. Figure 5(1) is the image in the MOT and Fig. 5(2) is the image at the end of the acceleration of $1\ \text{ms}$. Figure 5(3) is the image of the accelerated atomic cloud ($1\ \text{ms}$ of acceleration) followed by a free flight of $0.7\ \text{ms}$. Spatial profiles along the z axis and the x axis of each image are shown in Figs. 5a,b, respectively. The transverse spreading of the atomic cloud during the acceleration was 5% , which indicates that the transverse radiation pressure is effective after

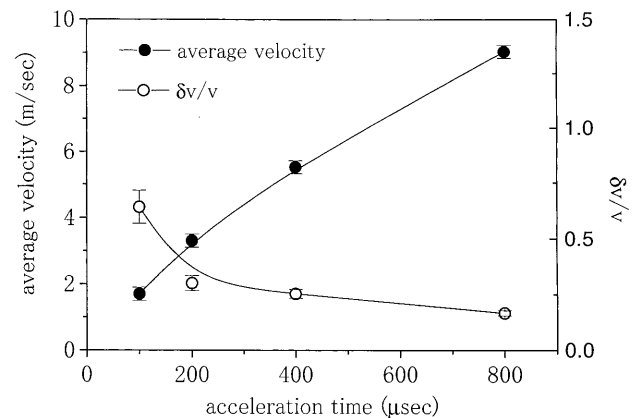


Fig. 4. The longitudinal average velocity v and the relative velocity spread $\Delta v/v$ as a function of acceleration time τ_a

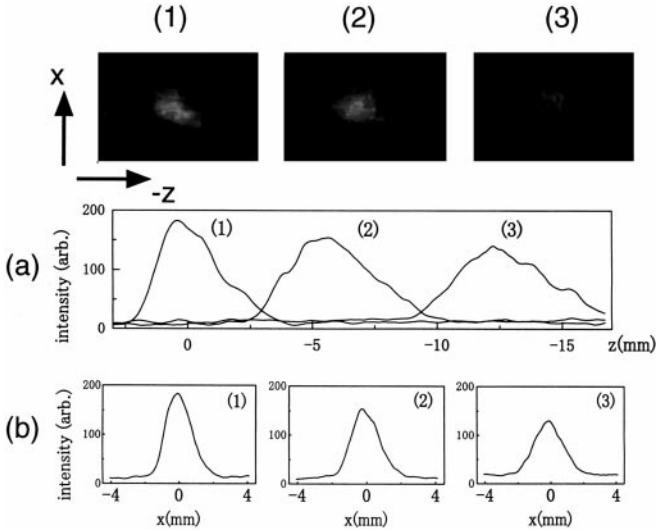


Fig. 5a,b. Fluorescence images of the atomic cloud at different times. (1) Atomic cloud in the MOT, (2) at the end of 1.0 ms of acceleration, (3) after 1 ms of acceleration, and 0.7 ms of free flight. The spatial profiles of each cloud along the z axis (a) and the transverse direction (b) are shown below

changing the downstream magnetic field to guide the atomic cloud like a funnel. The average velocities derived from the imaging data agree with the results from the TOF measurements. The maximum average velocity of 13 m/s was obtained after 1.2 ms of acceleration. The beam divergence of the accelerated atoms was derived from the imaging data. It was 47 ± 10 mrad.

To estimate the velocity of accelerated atomic cloud we numerically calculated a force on a two-level atom propagating in the negative z direction in the temporally varying magnetic field $B(z, t)$. The intensity profile of the laser beam is described as $I/I_0 G(z)$, where I_0 is the saturation intensity, I is the power density of one beam and $G(z)$ is the Gaussian profile. The average radiation-pressure force from one transverse laser beam in the z direction is described by the following equation:

$$F(z, t) = \hbar k \frac{\Gamma}{2} \times \frac{\frac{I}{I_0} G(z)}{1 + \frac{I}{I_0} G(z) + \left\{ \frac{(\omega_L - \omega_0) - \vec{k} \cdot \vec{v}(t) + \Delta(m_{FGF}) \mu_B B(z, t) / \hbar}{\Gamma/2} \right\}^2}, \quad (2)$$

where $\Gamma/2\pi$ is the natural line width of the transition, $\omega_L - \omega_0$ is the detuning of the trapping laser frequency from the resonance, $\vec{k} \cdot \vec{v}(t) = kv(t) \cos 70.5^\circ = kv(t)/3$ is the velocity-induced Doppler shift of the transition frequency, $\Delta(m_{FGF}) \mu_B B(z, t) / \hbar$ is the frequency difference of the Zeeman shift of upper and lower states.

In the numerical analysis of the present experiment, we used the values for the ${}^2S_{1/2}(F=2, m_F=-2) - {}^2P_{3/2}(F=3, m_F=-3)$, because atoms were pumped optically into the lowest magnetic sublevel by the sideband light. Then, the difference of m_{FGF} was 1. Other parameters in our experiment were $\omega_L - \omega_0 = -15$ MHz, $I/I_0 = 0.7$ and the Gaussian profiles with $1/e^2$ radius of 10 mm. The calculated average force in the z direction is shown in Fig. 6 as a function of the axial

distance z . Figure 6a shows the force when the quadrupole magnetic field of the MOT is kept constant. A center of the atomic cloud is initially at the position of $z = 0$ and the cloud moves toward the negative- z direction. Figure 6b shows the force when the current through the downstream coil decays exponentially with the time constant of 0.3 ms, which is our experimental condition, the rate of absorption of photons recovers and atoms are accelerated.

The time evolution of the velocity on the z axis was obtained by solving a simple equation of motion with the force described by (2). The calculated velocities at three decay constants, 1 ms, 0.3 ms, and 0.1 ms, are shown in Fig. 7. The experimental data are also shown in the figure by dots. The calculated final velocity at the decay constant of 0.3 ms was slightly higher than the velocity obtained in the experiment. The reason of this slight discrepancy may be that the atoms

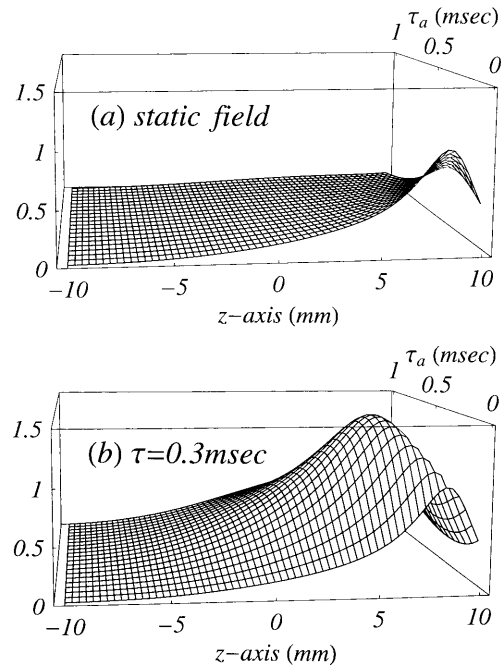


Fig. 6a,b. Calculated longitudinal average force on a moving atom. **a** The magnetic field is static quadrupole field. **b** The current of downstream coil decays exponentially with the time constant of 0.3 ms

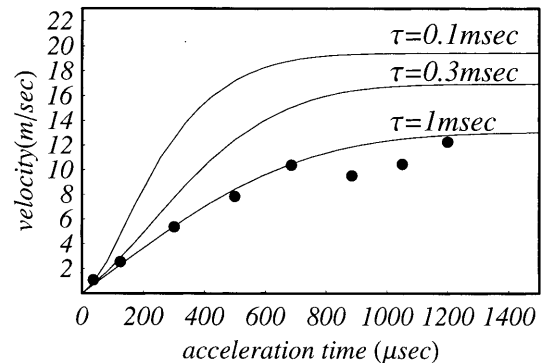


Fig. 7. The calculated time evolution of longitudinal average velocity (solid curves) and the experimental data (dark dots). The current of downstream coil decays exponentially with the time constants of 1 ms, 0.3 ms, and 0.1 ms, respectively

were optically pumped into another ground state hyperfine component $F = 1$ even though the repumping laser was used. The power density of the repumping beam was 1/3 of the trapping beam and 30% of atoms in our MOT were estimated to stay in the $F = 1$ level. The ratio of the population between the hyperfine levels in an accelerating atomic cloud would be the same as in the MOT. The calculation shows also that the decay time constant of the current in the trapping coil is an important parameter for the efficient acceleration of atoms. Final velocity of up to 20 m/s could be obtained if the current decayed within 0.1 ms. The laser power density and the beam diameter are also important parameters.

The flux and the brightness of the pulsed atomic beam were estimated from the fluorescence intensity of the atomic cloud and the beam divergence. A typical number of trapped atoms was 5×10^9 , and it gives the flux of 6.7×10^{12} atoms/s with 6.5 m/s average velocity and 1 ms pulse width. The velocity spread was 1.3 m/s. The brightness of the beam was 1.1×10^{15} atoms/sr.s. The repetition rate, which depends on the loading time of the MOT, is an important parameter when we use the pulsed atomic beam for various experiments. The repetition rate was 1 Hz in our experiment. A slow, intense, and velocity-controllable pulsed atomic beam is a powerful tool for collision experiments. This method can be applied to any atoms that can be trapped in a MOT. It should be noted that the atomic beam is free from the light field after they are released. Therefore, there is no ac-Stark shift of energy levels, which is essential in various high-precision measurements.

4 Conclusion

We have demonstrated a new technique to produce a SAB-NVS by accelerating atoms in a magneto-optical trap. The

three transverse trapping beams in the tetrahedral laser beam configuration accelerated atoms longitudinally and at the same time confined transversely resulting in the small beam divergence. The velocity of the pulsed atomic beam was varied up to 13 m/s by adjusting the acceleration time. All atoms in a MOT were accelerated to one direction and we obtained the flux density of as large as 1.1×10^{15} /sr.s. The experimentally obtained velocity distribution was fitted with the numerical calculation. The numerical calculations show also that the velocity control of the atomic cloud in a wider range is possible with the present technique.

Acknowledgements. We would like to acknowledge helpful discussions with Prof. H. Takuma, and we are grateful to Prof. F. Shimizu for technical advice. This work has been partly supported by the Grants in Aid for Scientific Research (11216202) from the Ministry of Education, Science, Sports and Culture.

References

1. W.D. Phillips, H. Metcalf: Phys. Rev. Lett. **48**, 596 (1982)
2. T.E. Barrett, S.W. Dapore-Schwartz, M.D. Ray, G.P. Lafyatis: Phys. Rev. Lett. **67**, 3483 (1991)
3. E. Riis, D.S. Weiss, K.A. Moler, S. Chu: Phys. Rev. Lett. **64**, 1658 (1990)
4. J. Nellesen, J. Werner, W. Ertmer: Opt. Commun. **78**, 300 (1990)
5. J. Yu, J. Djemaa, P. Nosbaum, P. Pillet: Opt. Commun. **112**, 136 (1994)
6. T.B. Swanson, N.J. Silva, S.K. Mayer, J.J. Maki, D.H. McIntyre: J. Opt. Soc. Am. B **13**, 1833 (1996)
7. A. Scholz, M. Christ, D. Doll, J. Ludwig, W. Ertmer: Opt. Commun. **111**, 155 (1994)
8. Z.T. Lu, K.L. Corwin, M.J. Renn, M.H. Anderson, E.A. Cornell, C.E. Wieman: Phys. Rev. Lett. **77**, 3331 (1996)
9. S. Weyers, E. Auccouturier, C. Valentin, N. Dimarcq: Opt. Commun. **143**, 30 (1997)
10. F. Shimizu, K. Shimizu, H. Takuma: Opt. Lett. **16**, 339 (1991)
11. J. Kawanaka, K. Shimizu, H. Takuma: Appl. Phys. B **57**, 113 (1993)